

# FEM modeling of an entire 5-IDT CRF/DMS filter

Victor Plessky, Julius Koskela  
GVR Trade SA  
Gorgier, Switzerland  
victor.plessky@gmail.com

B.A. Willemsen, P.J. Turner, Filip Iliev,  
R.B. Hammond, N.O. Fenzi  
Resonant Inc.  
Santa Barbara, California, USA

*Abstract* A CRF/DMS filter is simulated using “Layers” software [1-2]. We analyze a few different CRF/DMS structures, including the 10-port CRF device with passband frequency close to 1842.5 MHz including 5 IDTs, 8 “gap IDTs” and 2 reflectors. This TC SAW structure has a thick SiO<sub>2</sub> over layer covering 274 Cu electrodes on a 128° LiNbO<sub>3</sub> substrate. In addition to the electrical network parameters for the filter, a visualization of acoustic field and power flow is presented. The simulation reveals the resonances in the structure, radiation of energy at the interfaces between IDTs, and helps to see the origin of notches in passband including parasitic acoustic modes. We simulate 801 frequency points and present acoustic fields, power flows, and generated bulk waves inside the entire device for select frequencies of interest. On a PC with 32 processors and 128 GB RAM, a complicated device having 15 “building blocks” (274 electrodes) was simulated, with about 6 second simulation time per frequency point (~1.3 hours total time). Losses due to bulk wave generation are numerically estimated.

*Keywords*—CRF/DMS; FEM, leaky waves; bulk wave generation; loss mechanisms; 5-IDT CRF, power flow

## I. INTRODUCTION

Competitive SAW filter technology today includes different substrates, multilayered electrodes from *Al*, *Cu*, *Pt*, ..., dielectric sublayers and over-layers, etc. Temperature compensated SAW filters have been developed that have performance competitive with FBARs. Traditional design tools, such as those based on COM models, demand experimental characterization of wave propagation parameters. FEM/BEM models cannot be easily adopted to new substrates and calculations are slow. The advantage of FEM methods is their remarkable generality. FEM can handle arbitrary materials and crystal cuts, different electrode shapes, and structures including multiple metal and dielectric layers. The main challenge in applying FEM to SAW devices has been unacceptably long computation times. Recently, we proposed “hierarchical cascading” FEM software called “Layers” [1-2], suitable for simulating any 2D SAW device with many hundreds of electrodes with a speed of 1-7 seconds per frequency point on a 32 processor PC. Note that the cascading procedure does not imply any periodicity of acoustic/electric fields in the structure, or any additional approximations and exact acoustic and electric field distributions can be obtained for all FEM grid points of the

device. That gives us a unique possibility to look what happens inside such a device. Moreover, we can calculate the energy accumulated in the device and the power flow. Power flow of bulk and surface waves generated (scattered) in the device, and leaving it, is integrated on the boundary of the computational mesh. In this way, we can numerically estimate the level of loss associated with the bulk wave generation.

The recent remarkable progress in reducing loss in SAW filters achieved by Murata workers and Prof. M. Kadota with co-authors [3-6] is based, mainly, on suppression of bulk radiation losses. Here we study radiation losses in synchronous resonators, then in a kind of “hiccup” structure [7], in so-called “degenerated CRFs” [8], and, finally, in the popular CRF structure with 5 main IDTs.

## II. RADIATION PICTURES

### A. Synchronous resonator

Synchronous resonators are the main building blocks of the “ladder” filters, widely used in mobile phones, especially in TX parts of duplexers. It is believed that the periodicity of electrodes and absence of any gaps create favorable conditions for minimizing wave scattering on structural non-uniformities. However, our modeling shows that the ends of the IDT, even in completely periodic structure with the same period and form of electrodes in the IDT and reflectors, do radiate bulk waves (Fig.1). This radiation represents visible part of losses. It is interesting to note that even in IHP-like structures, similar to described in [5-6], some “edge of IDT” radiation losses are present (Fig.2), albeit very small in magnitude. Detailed analysis of the field distribution, accumulated SAW energy, and power flow in a synchronous resonator is presented in a parallel paper at this Symposium [8].



Fig. 1. Bulk radiation from the end of IDT: power flow in a synchronous resonator on 42°LiTaO<sub>3</sub> with light electrodes. Only the left half of the symmetric structure is shown.

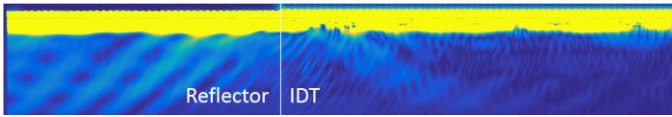


Fig. 2. Power flow in an IHP synchronous resonator, similar to described in [6]. Only the left half of the symmetric structure is shown. The bright part on top is shear-horizontal modes propagating in the active LiTaO<sub>3</sub> layer and the SiO<sub>2</sub>/AlN mirror. The light blue part is bulk waves emitted from the ends of the IDT and the reflectors into the Si substrate.

### B. “Hiccup”-like structure, leaky waves

Generally, term “CRF/DMS” may refer to very different structures, including more complicated mode structures than “double mode”. It is interesting to look inside a simple 2-IDT structure which we obtain by introducing a gap in the middle of a synchronous resonator. Such a “hiccup” [7] resonator was mainly used on ST-quartz.

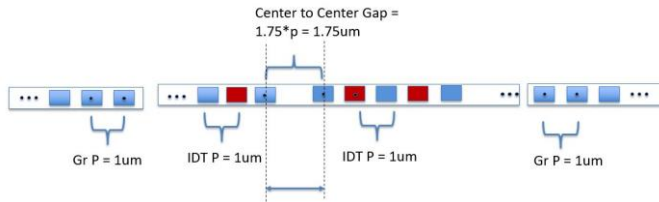


Fig. 3. “Hiccup” resonator geometry.

Here, we analyze a LSAW “hiccup” resonator on 42°YX-cut LiTaO<sub>3</sub>. The device has 2 resonances (see red curve in Fig.4): one at the left edge of stopband - which is just the resonance of the long transducers, and another resonance appears at the gap (Fig.5). The 2<sup>nd</sup> resonance appears not in the center of stopband because the gap of 1.75p is larger than necessary 1.5p for this type of resonator. One can see that the Q-factor of the resonator is too low (about Q=240), because of very strong losses of energy due to scattering of waves on the gap. The bottom part of Fig. 4 shows that the bulk wave radiation (see in Fig.6) is responsible for 90% of losses in this case at 2005 MHz.

Due to the high loss, this device is not used on leaky wave substrates. To illustrate the importance of the bulk wave scattering in the leaky wave devices, and power of our software, we have chosen here by far not the best design of the resonator. Replacing the gap by a “distributed gap” can significantly reduce the radiation loss. In the next section, we analyze such a device.

It is interesting to try a “hiccup” resonator on an IHP-type structure [5]. The device has an active 1 μm LiTaO<sub>3</sub> layer, and 500 nm thick SiO<sub>2</sub> and AlN reflector layers on top of a silicon substrate. Figure 7 shows that a lot of energy scattered at the gap penetrates the substrate. The simulated Q-factor of the resonance is about 400, limited essentially by BAW radiation.

### C. “Degenerated” CRF

Here we illustrate fields and power flow distributions in a simple 2-IDT CRF which is similar to the “hiccup” resonator

but two transducers are used as 2 ports, for input and output. Two resonances are present in the structure and, with correct

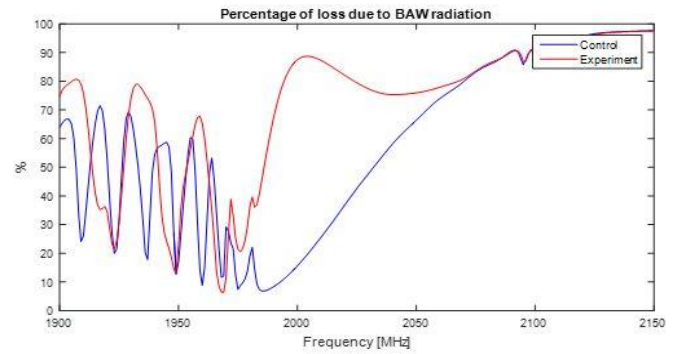
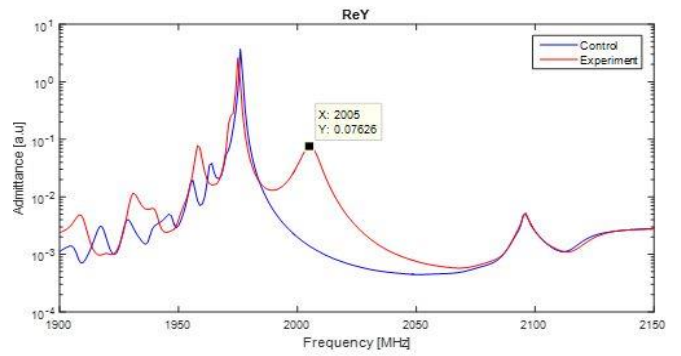


Fig. 4. Admittances (top) and the fractional bulk radiation loss (bottom).

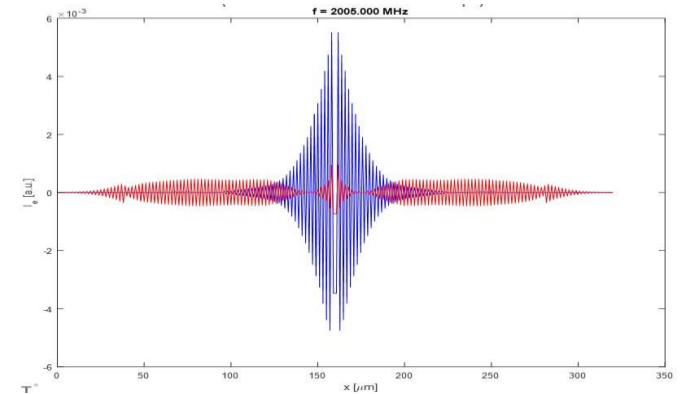


Fig. 5. Currents in the “hiccup” resonator. Blue and red curves correspond to real and imaginary part of current, when the input voltage phase is taken as reference.

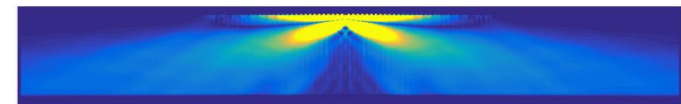


Fig. 6. Power flow in the “hiccup” resonator with 30+30 pairs of electrodes in the IDTs and a gap of 1.5p in the center of the structure.

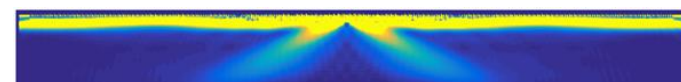


Fig. 7. Power flow in the “hiccup” resonator on IHP-like structure.

design, the resonance on the gap can be placed at the frequency corresponding to the anti-resonance of the long transducers [8] providing a kind of “self-matching” to the 50 Ohm load. The device included  $h/\lambda=8\%$  thick Al electrodes on  $42^\circ\text{LiTaO}_3$ , 15 pairs of electrodes in the IDT1 and 28 pairs in the IDT2 with the pitch close to  $2.7\ \mu\text{m}$ . In between these IDTs there was “distributed gap” of 6+6 electrodes having reduced pitch. The reflectors included 30 electrodes each, with the pitch a little wider than in the IDTs. Figure 8 shows the FEM-simulated filter response, which was close to the experimental results. The current distribution (Fig.9) illustrates rather complicated mode structure with the main resonance around the gap (broken periodicity). Figure 10 shows the main power flow in the device. We have calculated the voltages applied to these IDTs in a complete device loaded by 50/50 Ohm environment.

As expected, the main power flow is from IDT1 to the IDT2. However, the radiation from the ends of the IDTs is clearly visible. Although all flows are present together, with some imagination, one can see three types of radiation: shear bulk waves radiated by the ends of IDTs gliding at a small angle to the surface, leaky slow shear waves with the angle of propagation around  $45^\circ$ , and even some waves radiated from the interface between IDTs in the vertical direction. Numeric estimations show that the bulk acoustic wave radiation is responsible for about 57% of the losses in this device despite using the “accordion” distributed gap between the IDTs.

#### D. 5-IDT CRF, 8%Al on $42^\circ$ lithium tantalate

The geometry and key parameters of a more complex 5-IDT CRF are summarized in Fig. 11. The device was simulated under excitation of IDT T1 connected in parallel, with IDTs terminated with  $50\ \Omega$  impedance. The transfer function is shown in Fig. 12. The energy density stored within the device at selected frequencies is shown in Fig. 13, and the corresponding power flows in Fig. 14. The first and last frequency points are outside the stopband; the remaining five are at local minima and maxima within the stopband. One can note the lack of energy confinement outside the stopband, and the concentration of energy at the transducer edges within the stopband. The role of acoustic radiation in the total power loss increases steadily with frequency, from about 20% at 1540 MHz to greater than 90% at 1700 MHz. The radiation is seen to be strongly focused at the IDT-IDT and IDT-reflector boundaries.

#### E. 5-IDT CRF, TCSAW

Here, we consider a similar 5-IDT /10-port CRF (one of the test devices, not optimized) designed using a TCSAW approach on  $128^\circ$  lithium niobate with Cu electrodes and  $\text{SiO}_2$  layer with flattened top. The device includes 5 main IDTs with a pitch of  $2p \approx 1.90\ \mu\text{m} - 1.93\ \mu\text{m}$  and the transducers were separated by “gap IDTs”, including 10+10 electrodes having reduced pitch.

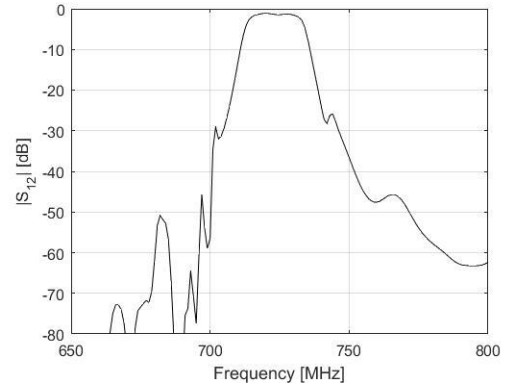


Fig. 8. 2-IDT CRF transfer function. Two tracks were connected using 2nd IDTs.

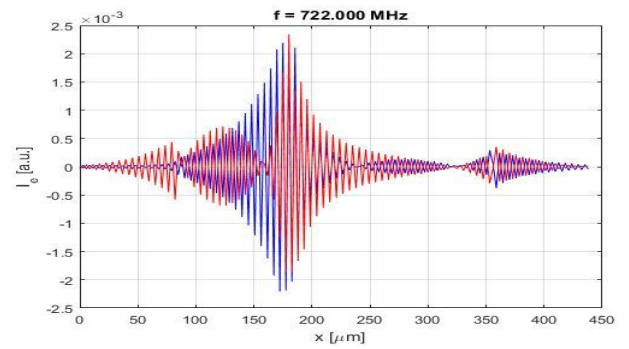


Fig. 9. Currents in 2-IDT CRF; middle of passband.

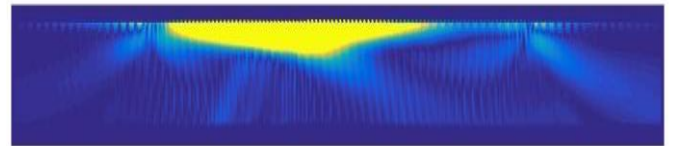


Fig. 10. Total power flow in 2-IDT CRF; middle of passband (722MHz).

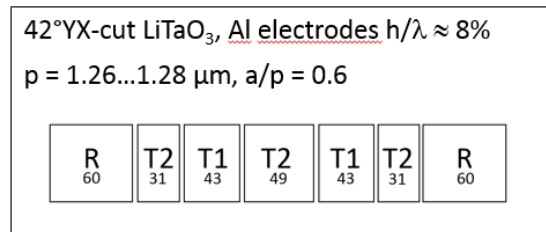


Fig. 11. Schematical structure and main parameters of the 5-IDT CRF.

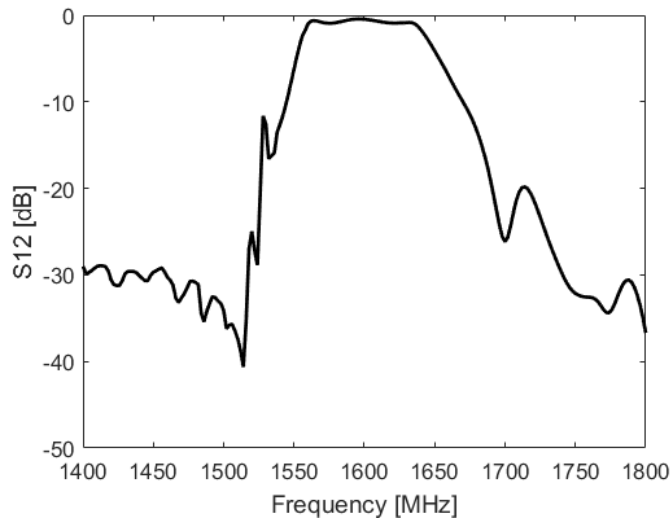


Fig. 12. Simulated transfer function of a 5-IDT CRF .

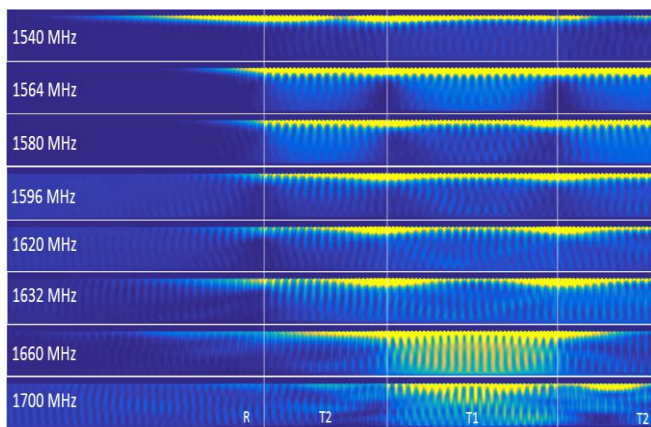


Fig. 13. Energy density in the 5-IDT CRF at selected frequencies below, within, and above the stopband. For better quality of visualization, only one half of the (symmetric) device is shown. All frequencies are presented using the same color scale.

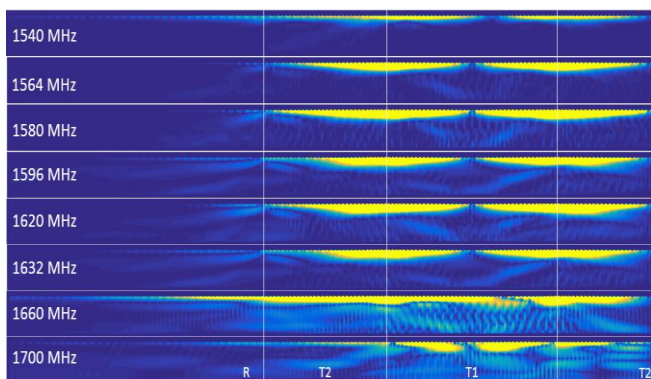


Fig. 14. Power flow in the 5-IDT CRF at various frequencies. For better quality of visualization, only one half of the (symmetric) device is shown.

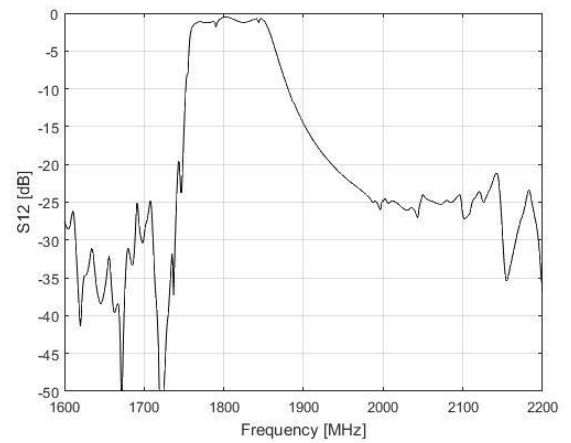


Fig. 15. Simulated transfer function of a 5-IDT CRF (TCSAW technology).

For this complicated device having 15 building locks in total with periodic electrode structure (274 electrodes in total) the frequency response (Fig. 15) was calculated in 801 frequency point with calculation time of 6.2 seconds per point. Fig. 16 shows the current distribution at 1800 MHz, corresponding to the frequency of minimal loss in passband. Compared to the leaky wave case (Fig.4) we see almost no bulk radiation. The device operates using Rayleigh-type SAW, which are not as sensitive to the gaps, and bulk waves are responsible only for about 2% of total loss. However, some radiation can be seen from the gap between the reflector and the first IDT (Fig. 17). No “distributed” gap was applied in that case.

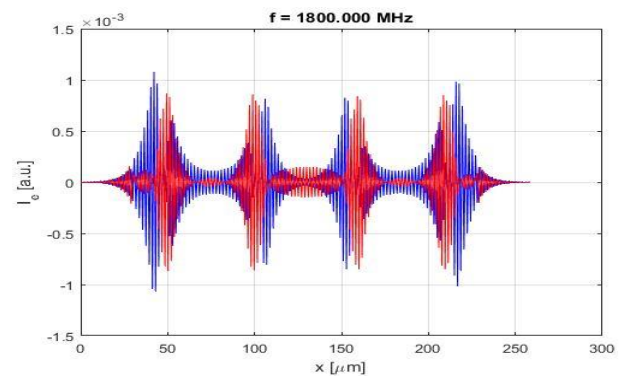


Fig. 16. Current distribution in 5-IDT CRF (TCSAW technology).

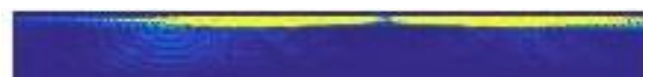


Fig. 17. Power flow in 5-IDT CRF (TCSAW technology).

It is clear that obtaining the complete field and energy distribution/flow demands much more computation time than just the admittance calculations. The images shown here, although strongly averaged, have big volume of >100MB in initial MATLAB \*.fig format.

### III. DISCUSSION

The possibility to “look” inside simulated devices and to see the complete details of energy distributions and flows gives us better understanding of loss mechanisms. Figures 13-16 show that in the 5-IDT CRF we have a complicated distribution of SAW amplitudes with the resonances mainly being concentrated around the gaps between the IDTs. Although we have not demonstrated it here, by changing the outside impedances the resonances can be separated and studied/visualized separately. For example, for the notch in the passband near 1790 MHz (Fig. 15), the current distribution looks perturbed (Fig. 18). We see (Fig.19) that the resonances are not of equal intensity and the main energy is concentrated only at the gaps between the center IDT and its neighbors.

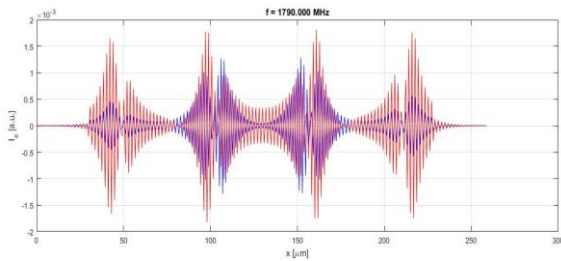


Fig. 18. Current distribution at the notch frequency

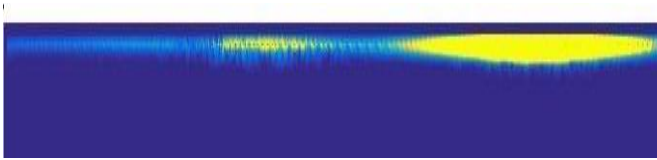


Fig. 19. Power flow at the notch frequency.

### IV. CONCLUSIONS

We have demonstrated that our FEM software “Layers”, which is based on cascading sections in SAW devices having block structure with periodic electrodes inside blocks, such as CRF/DMS, can be used for visualization of acoustic/electric fields inside all points of studied devices, including visualization of accumulated energy, power flows and numeric estimation of losses caused by the bulk wave radiation. We have a powerful tool for understanding the physics of device operation and for minimization of the losses related to the bulk wave radiation.

### ACKNOWLEDGMENT

One of the authors (VP) is grateful to O. Losev, A. Shimko, M. Solal, V. Yantchev, M. Kadota for discussions of the physics of SAW devices.

### REFERENCES

[1] Koskela, J., Maniadis, P., Willemsen, B. A., Turner, P. J., Hammond, R. B., Fenzi, N. O., & Plessky, V. (2016, September). “Hierarchical

cascading in 2D FEM simulation of finite SAW devices with periodic block structure”. In Ultrasonics Symposium (IUS), 2016 IEEE International (pp. 1-4). IEEE.

[2] J. Koskela, V. Plessky, P. Maniadis, P. Turner and B. Willemsen, “Rapid 2D FEM Simulation of Advanced SAW Devices”, TH02C\_4, in Proc. of IMS, 2017, Honolulu, Hawaii.

[3] Kadota, Michio, and Shuji Tanaka. “Solidly mounted ladder filter using shear horizontal wave in LiNbO<sub>3</sub>.” Ultrasonics Symposium (IUS), 2016 IEEE International. IEEE, 2016.

[4] Takai, Tsutomu, et al. “Incredible high performance SAW resonator on novel multi-layered substrate”, Ultrasonics Symposium (IUS), 2016 IEEE International. IEEE, 2016.

[5] Takai, Tsutomu, et al. “High Performance SAW Resonator on New Multi-layered Substrate using LiTaO<sub>3</sub> Crystal.” IEEE Transactions on Ultrasonics, Ferroelectrics, and Frequency Control (2017), to be published.

[6] M. Kadota and S. Tanaka, “HAL SAW Resonators Using LiTaO<sub>3</sub> Thin Plate on Quartz Substrate”, in Freq. Control Symposium, Besançon, 2017.

[7] Wright, P. V. “A review of SAW resonator filter technology.” Ultrasonics Symposium, 1992. Proceedings., IEEE 1992. IEEE, 1992.

[8] Meltaus, J., Hong, S. S., Holmgren, O., Kokkonen, K., & Plessky, V. P. (2007). Double-resonance SAW filters. *IEEE transactions on ultrasonics, ferroelectrics, and frequency control*, 54(3).

[9] V. Plessky, J. Koskela, B. A. Willemsen, P. J. Turner, R. B. Hammond, N. O. Fenzi, “Acoustic Radiation from Ends of IDT in Synchronous LSAW Resonators”, this Symp., unpublished.